

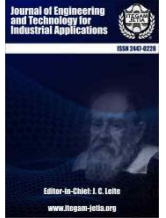


ISSN ONLINE: 2447-0228

ITEGAM-JETIA

Manaus, v.10 n.47, p. 83-94. May/June., 2024.

DOI: <https://doi.org/10.5935/jetia.v10i47.1098>



RESEARCH ARTICLE

OPEN ACCESS

DYNAMICS ASSESSMENT OF AN INVERTER FED INDUCTION MOTOR DRIVE BY AN IMPROVED PREDICTIVE CONTROLLER LEVERAGING FINITE CONTROL SET MECHANISM

Shaswat Chirantan*¹, Dr. Bibhuti Bhusan Pati²

¹PhD. Scholar, Department of Electrical Engineering, Veer Surendra Sai University of Technology, Burla, Sambalpur, 768018, India.

²Department of Electrical Engineering, Veer Surendra Sai University of Technology, Burla, Sambalpur, 768018, India.

¹<http://orcid.org/0000-0001-9052-3582>, ²<http://orcid.org/0009-0009-3897-5712>

Email: *shaswat.chirantan443@gmail.com, bbpati_ee@vssut.ac.in

ARTICLE INFO

Article History

Received: April 09th, 2024

Revised: June 03th, 2024

Accepted: June 18th, 2024

Published: July 01th, 2024

Keywords:

Model Predictive Control, Predictive Current Control, Finite Control Set, Integral Finite Control Set, Induction Motor.

ABSTRACT

Accenting the importance of Model Predictive Control (MPC) across used optimization tools in current engineering applications, the proposed scheme establishes the predictive skills by well-defined mathematical model in terms of present state variables. This paper projected a predictive current control (PCC) approach scheduled by finite control set (FCS) inverter switching mechanism executed by a current modulated objective function. The anatomy of this controller deals with selecting the control signal from a finite set of signals which satisfies minimum value of the predefined objective function, which is formulated by calculating the square error, i.e. the reference current against the stator measured current of the designed induction motor (IM). The proposed work further enriched with an improved predictive aspect named as integral finite control set (IFCS) action synchronized with a cascade feedback structure with appropriate controller gain to obtain an optimal set of control variables. With the direction in minimization of principle, these methods provide the control of the switching states for inversion, to the inverter and inverter generates actuating voltage signals to the induction motor. IFCS-MPC has the inherent capabilities of compensating steady state errors and slewrates which portrayed this as the preferred forecasted controller as compared to FCS-MPC. This work is also advanced with a comparative demonstration of torque, load currents and speed characteristics of IM, obtained from each of the implemented control techniques to identify the most flexible and dynamic predictive strategy. All these control methods have been investigated using MATLAB/Simulink environment.



Copyright ©2024 by authors and Galileo Institute of Technology and Education of the Amazon (ITEGAM). This work is licensed under the Creative Commons Attribution International License (CC BY 4.0).

I. INTRODUCTION

In electrical field, MPC has been more effective to utilize and the control the switching of power converters, synchronous and induction machine drives and for various power system parameters control. Wide range of predictive control algorithms have been implemented by many researchers. MPC has received widespread attention due to its flexibility, robustness and fast dynamic responses. MPC topology can be categorized in to analogous mode, i.e. continuous control set (CCS) and discrete mode, i.e. finite control set (FCS), depending on their operation and control actions.

Predictive current control schemes for power converters and electrical drives have been proposed in [1], which demonstrates CCS-MPC algorithm, receding horizon control principle with forward Euler approximation and cost function for discrete time load model of PMSM (permanent magnet synchronous motor) for switching states of the inverter. The introduction of Integral FCS is to minimize the steady state error those cannot be significantly reduced by FCS. Implementation of IFCS in AC motor drive to analyze the steady state error in d & q axis currents has been presented in [2]. Earlier to the evolution of MPC techniques conventional controllers such as PI, PD, PID have been used widely.

In [3], the algorithms of FCS & IFCS MPC topologies to control various synchronous and asynchronous motor drives have been designed and compared with conventional controllers. A new FCS MPC technique to regulate the flux dynamics of an Induction Motor is proposed [4]. In this control approach, to minimize the problems associated with switching frequency PWM technique is implemented. A comparative study between FCS & CCS method has been highlighted in [5]. This work discussed the execution methodology of both FCS & CCS action such as modulation control and SVPWM control scheme respectively. Predictive control strategy of an inverter fed IM drive can be designed with current evaluation or with flux/torque evaluation [6]. This study provides the practical perception of MPC for converter fed drive systems. In order to diagnose the performance of IM various strategies have been incorporated, considering the field oriented control, with the direct torque control and the predictive controllers [7]. Basically optimization problems are assigned with specific cost functions depending on system parameters. To achieve fast dynamic behaviour of Induction machine an innovative control strategies with two different objective functions have been defined for both torque and flux respectively [8]. A MPC scheme has been proposed in [9] to direct flux control of multi-three phase structure induction motor for improvement of the fault tolerant behavior of the drives by independently controlling the three phases. IFCS MPC strategy for a single phase Z-source inverter has been implemented in [10] to compensate the steady state error caused by FCS method.

II. RELATED WORKS

FCS MPC is found to be a promising control method for converter fed IM drive. Two case studies of inverter fed induction machine with and without LC filter have been analyzed in [11]. A predictive control approach is proposed in [12] to determine the length of control horizon of an induction motor drive. As already discussed in the earlier literature, predictive control can be a fast-acting action for optimal control of inverter switching states [13]. Generally finite control set based controller provides fast dynamic response and overcomes the limitations of conventional PI controller. In [14], a deadbeat FCS predictive current control topology has been proposed for enhancing the IM dynamics. The adaptability, robustness and flexibility of FCS technique has been compared with classical controllers [15] and a sliding mode based MPC method has been introduced for torque and flux control of induction motor [16]-[17]. Field oriented control of a three-phase induction motor by constraints incorporated FCS-MPC method with direct current control strategy is demonstrated in [18]. Through this algorithm the deviations between desired currents and predicted currents can be minimized. Apart from single or three phase IM, predictive mechanism has also provided a genuine control algorithm for multi-phase machines such as five phase or six phase [19]-[21] to optimize the machine performances. To regulate the phase angles of stator phase currents a predictive phase angle controller has been assigned [22] and overall machine characteristics have been analyzed. The main aspects of controlling the induction machine dynamics are to monitor the flux and current behaviour. Accordingly, an observer based predictive flux control [23] and various current control [24]-[25] strategies have been implemented to observe and control the machine parameter variations. The development of MPC methods has been growing in much faster rate due to its reputation of quick response and simple system algorithm. Many advantages of this novel technique include current and torque harmonic distortion minimization [26], multiple

objectives optimization and fast fault tolerant approach [27]. In current scenario, predictive controllers are significantly used in high performance drives systems such as Induction machine, Synchronous machine, linear motors, reluctance motors and multi-phase machine drives [28]. A total disturbance observer-based PCC model of IM has been presented in [29], which takes the disturbance directly in the prediction mechanism and hence eliminates the need of a separate controller. The recent advancement of MPC action has the fast-acting control mechanism of multi-phase induction motor drives [30]-[33]. Application of model predictive control in power electronics enhances the flexibility, robustness and fastness of designed control architectures. For increasing dynamics, different predictive controllers are used such as deadbeat, hysteresis current controller (HCC) and trajectory-based controllers. Predictive controllers of machine drives are based on current or torque/flux control [34]-[35]. Although FCS-MPC method applied by researchers has mostly improved the dynamic response of the system, the technique has drawbacks in regard to the steady state error minimization. Hence this work is motivated to apply finite control set model predictive control (IFCS-MPC) with integral action to keep minimizing the steady state error and with fast dynamic response. Therefore, two integral gain constants K_d and K_q for direct & quadrature axis currents are introduced in the control structure respectively. Hence it is required to have a proper value of these two parameters to obtain the system with minimum steady state error and acceptable switching losses. Further, intelligent techniques also used for machine control [36].

The detailed case studies of the implemented techniques have been thoroughly analyzed. The remainder of the article is organized as follows. Section 2 demonstrates the inverter topology, dynamic model, control methodologies and algorithms involved to designed the proposed predictive controllers for a IM drive. Section 3 plots and discusses the responses of torque, currents and speeds with respect to step changes of various control action proposed. Section 4 sites the performance comparison of designed MPCs in terms of torque and current dynamic characteristics. And finally, Section 5 concludes the paper.

III. PROPOSED MODEL AND CONTROL METHODS

The working principle of the Model predictive control (MPC), where the variable of interest is control for the, predicted for finite horizon and compares with desired reference value to get the required command signal. This proposed work is based on simplification of inverter states optimization without any PWM technique. Here eight combinations of inverter states are formed as constraints to the control design. The load model is taken into action for the better prediction of the future behavior, the variables so the name model predictive control arises. The optimization technique works with receding horizon control principle. We can say that a constraint free FCS-MPC method is similar to the discrete time deadbeat feedback control system in which the controller gain is varies with time with the condition that closed loop poles are located at the origin of the complex plane. To improve the steady-state behavior of the normal FCSMPC method an integral action is added via a cascade control structure. The objective function for minimization in normal FCS-MPC method is just the square difference between predicted current and measured current in d-q reference fame. The main utility of the objective function in a I-FCS-MPC method, is explicitly related with the sampling time Δt .

III.1 MPC METHODOLOGY

MPC works with a finite-horizon control principle. The controller or MPC block makes evaluation of control signals for a definite future time. As the time passes the finite predictive horizon get updates by including a future time span and leaving a past time span. Based on the predicted output of the plant, MPC generates a control sequence which is applicable only at the current time sampling. After one sampling interval, the control sequence get modified based on the new measured variables. (Figure 1).

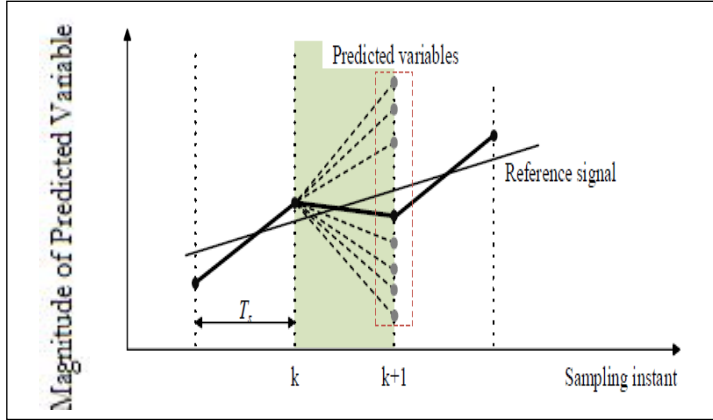


Figure 1: MPC Methodology.
Source: [3].

In Figure 1, the red trajectory is the reference signal which is to be followed. The green trajectory is the controlled signal obtained after due measurements and manipulation at the time instant k. The yellow curve is the past measured variable which is used for making the prediction for the future. At the current state k, the MPC evaluates the control sequence for the prediction horizon as indicated by the purple line. Similarly at the sampling instant k+1, k+2 etc., MPC generates different sets of controlled sequence for there respective prediction horizon.

This proposed work is based on simplification of inverter states optimization with out any PWM technique. Here eight combination of inverter states are formed as constraints to the control design. A load model is used to predict the future behaviour of the variables so the name model predictive control arise. The optimization technique works with receding horizon control principle. We can say that a constraints free FCS-MPC method is similar to the discrete time deadbeat feedback control system in which the controller gain is varies with time with the condition that closed loop poles are located at the origin of the complex plane. To improve the steady-state behaviour of the normal FCS-MPC method an integral action is added via a cascade control structure. The objective function for minimization in normal FCS-MPC method is just the square difference between predicted current and measured current with respect to the d-q referral fame, whereas explicitly related with the sampling time Δt , in the I-FCS-MPC method.

III.2 DYNAMIC MODEL OF INDUCTION MOTOR

For our experimental setup in a simulation environment, we have taken a case of a squirrel cage type, induction motor. The current and torque dynamics are represented in following mathematical equations with respect to the d-q referral frame [3].

$$\frac{di_{sd}}{dt} = -\frac{1}{\tau_{\sigma}}i_{sd} + \omega_s i_{sq} + \frac{k_r}{r_{\sigma}\tau_{\sigma}\tau_r}\varphi_{rd} + \frac{1}{r_{\sigma}\tau_{\sigma}} \quad (1)$$

$$\frac{di_{sq}}{dt} = -\omega_s i_{sd} - \frac{1}{\tau_{\sigma}}i_{sq} - \frac{k_r}{r_{\sigma}\tau_{\sigma}}\omega_e \varphi_{rd} + \frac{1}{r_{\sigma}\tau_{\sigma}} \quad (2)$$

$$\omega_s = \omega_e + \frac{L_h}{\tau_r} \quad (3)$$

$$\omega_s = \omega_e + \frac{1}{\tau_r} \frac{i_{sq}}{i_{sd}} \quad (4)$$

Where

i_{sd} & i_{sq} are the measured currents in d-axis, q-axis, expressed in Ampere (A)

v_{sd} & v_{sq} are the measured currents in d-axis, q-axis, expressed in Volt (V)

ω_s, ω_e are the angular speed of the stator and rotor, expressed in rad/sec

φ_{rd} = Rotor flux of d-axis (Wb)

All other parameters used in the dynamic equations of IM drive are defined below.

Leakage factor:

$$\sigma = 1 - \frac{L_h^2}{L_s L_r} \quad (5)$$

Stator time constant:

$$\tau_s = \frac{L_s}{R_s} \quad (6)$$

Rotor time constant:

$$\tau_r = \frac{L_r}{R_r} \quad (7)$$

Coefficients:

$$k_r = \frac{L_h}{L_r} \quad (8)$$

$$r_{\sigma} = R_s + R_r k_r^2 \quad (9)$$

$$\tau_{\sigma} = \frac{\sigma L_s}{r_{\sigma}} \quad (10)$$

The torque generated due to magnetic field, commonly known as electromagnetic troque, is proportional to, the $\varphi_{rd}i_{sq}$, which is expressed as

$$T_e = \frac{3}{2} Z_p \frac{L_h}{L_r} \varphi_{rd} i_{sq} \quad (11)$$

The mechanical parametric of the induction motor need to be consider and derived from the general motor equation for rotation, which is given as follows,

$$J_m \frac{d\omega_m}{dt} + f_d \omega_m = T_e - T_L \quad (12)$$

Where $\omega_m(t)$, the mechanical velocity of the rotor ($\omega_m = \frac{\omega_e}{Z_p}$), J_m , inertia of the motor, f_d , the friction coefficient, T_e & T_L are the torque in the electromagnetic Field and the load, respectively. With

consideration of the dynamics, the model and using the above in to the motion equation, representing in (12),

$$\frac{d\omega_m}{dt} = \frac{-f_d}{J_m} \omega_m + \frac{3 Z_p L_h}{2 L_r J_m} \varphi_{rd} i_{sq} - \frac{T_L}{J_m} \quad (13)$$

The velocity of the rotor in the electrical field can express as follow,

$$\frac{d\omega_e}{dt} = \frac{-f_d}{J_m} \omega_e + \frac{3 Z_p^2 L_h}{2 L_r J_m} \varphi_{rd} i_{sq} - \frac{Z_p T_L}{J_m} \quad (14)$$

The physical and technical parameters defined, and used earlier in the IM model have been consider and tabulated below for system performance evaluation.

Table 1: 3-Φ IM model parameters.

Parameters	Values
Winding resistance offer to Stator (R_s)	11.2 Ohms
Winding resistance offer to Rotor (R_r)	8.3 Ohms
Winding inductance offer by Stator (L_s)	0.6155 Henrys
Winding inductance offer by Rotor (L_r)	0.6380 Henrys
Mutual inductance of Machine (L_h)	0.57 Henrys
Moment of inertia (J_m)	0.00176 kg-meter square
Friction viscous gain (f_d)	0.00038818 newton meter per radian per second
Number of Pole pairs (Z_p)	2nos

Source: [3].

III.3 THREE PHASE INVERTER MODEL

We consider a 3-φ inverter, which convert 520V to 3-φ AC, for a induction motor of squirrel cage type, whose physical parameter are mention in the Table 1. The operation of the inverter, in the mode of, a non-linear discrete time system and having 180° mode of operation, with 7 number of output & 8 number of configuration state. For simplicity and rounding off, in the modeling and mathematical calculation on simulation we ignore the IGBT saturation voltage, and diode forward voltage drop. The schematic power circuit as the voltage source, inverter to the 3-φ IM is given below in Figure 2.

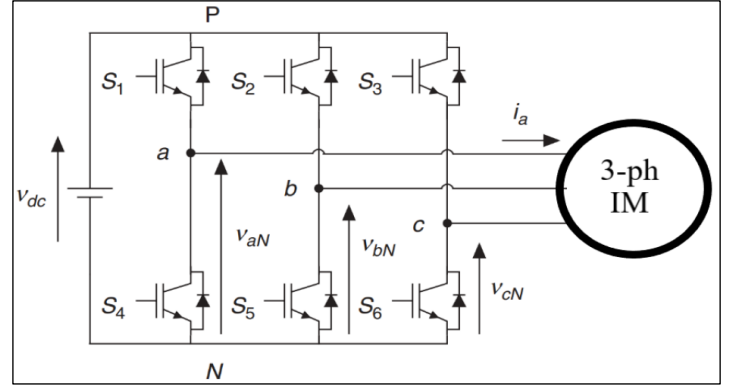


Figure 2: VSI fed 3-ph IM. Source: Authors, (2024).

The switching state for conversions is carryout with the reference of the gating signals S_a, S_b and S_c , and represented as follows [1]:

$$S_a = \begin{cases} 1, & \text{if } Switch_1 \text{ on and } Switch_4 \text{ off} \\ 0, & \text{if } Switch_1 \text{ off and } Switch_4 \text{ on} \end{cases}$$

$$S_b = \begin{cases} 1, & \text{if } Switch_2 \text{ on and } Switch_5 \text{ off} \\ 0, & \text{if } Switch_2 \text{ off and } Switch_5 \text{ on} \end{cases}$$

$$S_c = \begin{cases} 1, & \text{if } Switch_3 \text{ on and } Switch_6 \text{ off} \\ 0, & \text{if } Switch_3 \text{ off and } Switch_6 \text{ on} \end{cases}$$

The concept of space vector modulation [33] has been adopted for voltage vector with respect to optimum switching states. The generation of switching states, give rise to eight voltage vectors provided in Table 2 which can be predicted by Equation (15) as follows:

$$v = \frac{2}{3} V_{dc} (S_a + a S_b + a^2 S_c) \quad (15)$$

Where,

$a = e^{-j(2\pi/3)} = -\frac{1}{2} + j\frac{\sqrt{3}}{2}$, with a phase displacement of 120° between any two phases.

Table 2: Switching states with voltage vectors.

1	0	0	$\vec{v}_0 = 0$
1	0	0	$\vec{v}_1 = \frac{2}{3} V_{dc}$
0	1	0	$\vec{v}_2 = \frac{1}{3} V_{dc} + j\frac{\sqrt{3}}{3} V_{dc}$
0	1	0	$\vec{v}_3 = -\frac{1}{3} V_{dc} + j\frac{\sqrt{3}}{3} V_{dc}$
0	1	1	$\vec{v}_4 = -\frac{2}{3} V_{dc}$
1	0	1	$\vec{v}_5 = -\frac{1}{3} V_{dc} - j\frac{\sqrt{3}}{3} V_{dc}$
1	0	1	$\vec{v}_6 = \frac{1}{3} V_{dc} - j\frac{\sqrt{3}}{3} V_{dc}$

Source: Authors, (2024).

The simple mathematical model of three phase inverter circuit which defines the generated output voltages (phase to neutral) by means of switching signal application has been depicted

in Figure 3. The optimum operational of predictive algorithms, gives arise the switching state listed as above.

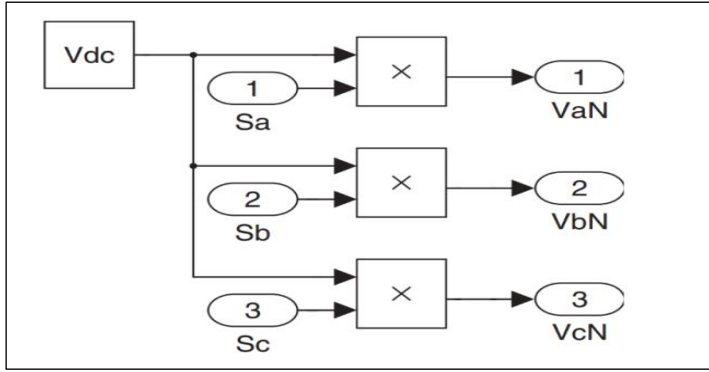


Figure 3: Ouput Voltage of VSI.
Source: Authors, (2024)

III.4 GENERALIZED PREDICTIVE CURRENT CONTROL ALGORITHM

Predictive current control algorithm can be states as:

1. The measurement of the reference current, $i^*(t_{i+1})$ is done from the outer control loop, whereas the load current $i(t)$

measurement need to be carryout at every states with respect to sampling interval.

2. The evaluation and prediction of the load current value for each upcoming sampling interval $i(t_{i+1})$, with considering the different voltage vector in consideration.

3. The cost function J deploy for the error calculation, difference of the reference against predicted currents, with each upcoming sampling frame with corresponding voltage vector.

$$J = \{i_d^*(t_i) - i_d(t_{i+1})\}^2 + \{i_q^*(t_i) - i_q(t_{i+1})\}^2 \quad (16)$$

4. The switching state signals, are generated minimizes the current error, are need to listed and consider for utilization.

In this algorithm the previous value the load current and the next state of the current, leads to predict 7 different states and 8 configurations, for operation of the inverter switching. For each discrete state, we need to calculate, the predict current value and compare, with the reference current for minimal error and changes. We need to calculate for all 8 stated as table above and record the errors. The optimal operational states are feed to the inverter, which used as voltage source. The flow diagram of the above process is shown in the Figure 4.

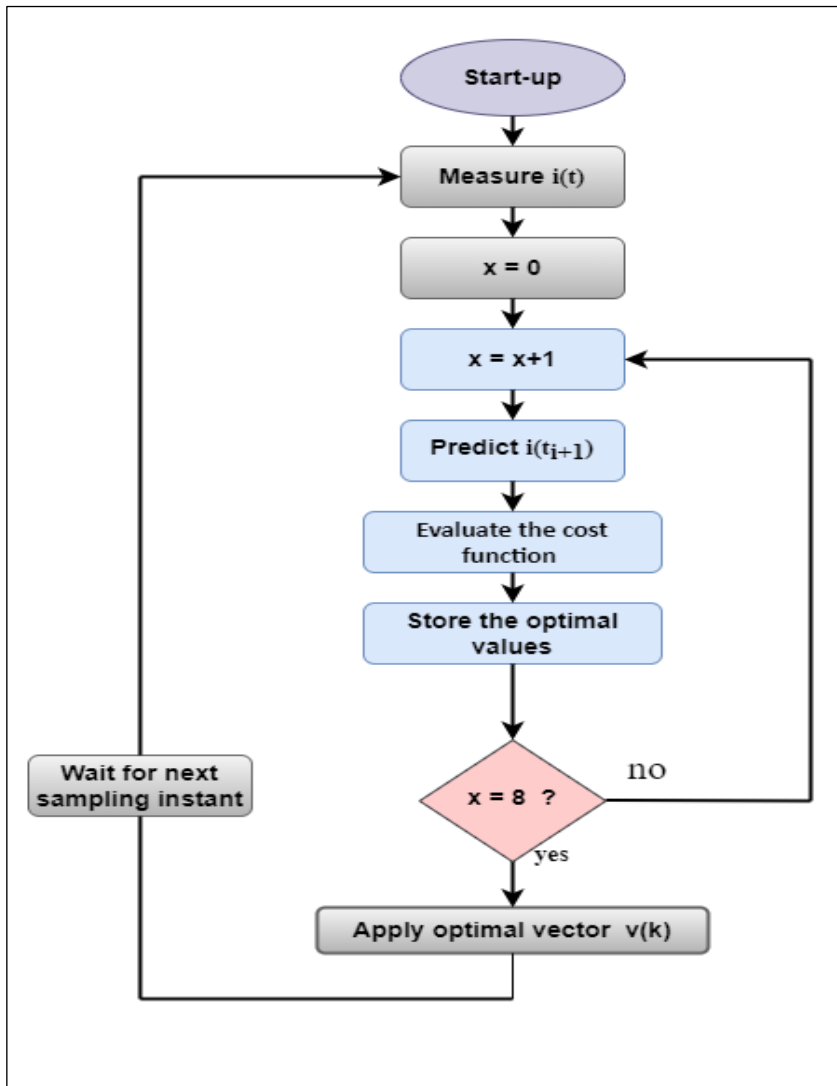


Figure 4: Flow Chart for PCC.
Source: Authors, (2024).

III.5 FCS-MPC SCHEME FOR IM

On generalization of equations, predicted load currents in d-q frame for sampling time t_i can be derived from forward Euler Approximations [1].

$$\frac{di_{sd}(t)}{dt} \approx \frac{i_{sd}(t_{i+1}) - i_{sd}(t_i)}{\Delta t} \quad (17)$$

i_d^* and i_q^* are the desired values of current in d-q frame.

Now by using Equations (17) & (18) in Equations (1) & (2) respectively, The discrete differential equations become the difference equations and can be represented as follows:

$$i_{sd}(t_{i+1}) = i_{sd}(t_i) + \Delta t \left(-\frac{1}{\tau_\sigma} i_{sd}(t_i) + \omega_s i_{sq}(t_i) + \frac{k_r}{r_\sigma \tau_\sigma \tau_r} \varphi_{rd}(t_i) + \frac{1}{r_\sigma \tau_\sigma} u_{sd}(t_i) \right) \quad (19)$$

$$i_{sq}(t_{i+1}) = i_{sq}(t_i) + \Delta t \left(-\omega_s i_{sd}(t_i) - \frac{1}{\tau_\sigma} i_{sq}(t_i) - \frac{k_r}{r_\sigma \tau_\sigma} \omega_e(t_i) \varphi_{rd}(t_i) + \frac{1}{r_\sigma \tau_\sigma} u_{sq}(t_i) \right) \quad (20)$$

The discretized prediction equations corresponding to Equation (19) and (20) are also presented in matrix form.

$$\begin{bmatrix} i_{sd}(t_{i+1}) \\ i_{sq}(t_{i+1}) \end{bmatrix} = (I + \Delta t A_m(t_i)) \begin{bmatrix} i_{sd}(t_i) \\ i_{sq}(t_i) \end{bmatrix} + \Delta t B_m \begin{bmatrix} u_{sd}(t_i) \\ u_{sq}(t_i) \end{bmatrix} + \begin{bmatrix} \frac{k_r \Delta t}{r_\sigma \tau_\sigma \tau_r} \varphi_{rd}(t_i) \\ -\frac{k_r \Delta t}{r_\sigma \tau_\sigma} \omega_e(t_i) \varphi_{rd}(t_i) \end{bmatrix} \quad (21)$$

Where,

I is a 2*2, identity matrix and

$$A_m(t_i) = \begin{bmatrix} -\frac{1}{\tau_\sigma} & \omega_s(t) \\ -\omega_s(t) & -\frac{1}{\tau_\sigma} \end{bmatrix} ; \quad B_m = \begin{bmatrix} \frac{1}{r_\sigma \tau_\sigma} & 0 \\ 0 & \frac{1}{r_\sigma \tau_\sigma} \end{bmatrix}$$

The structure of FCS-MPC Model used for 3-ph induction motor is presented in Figure 5.

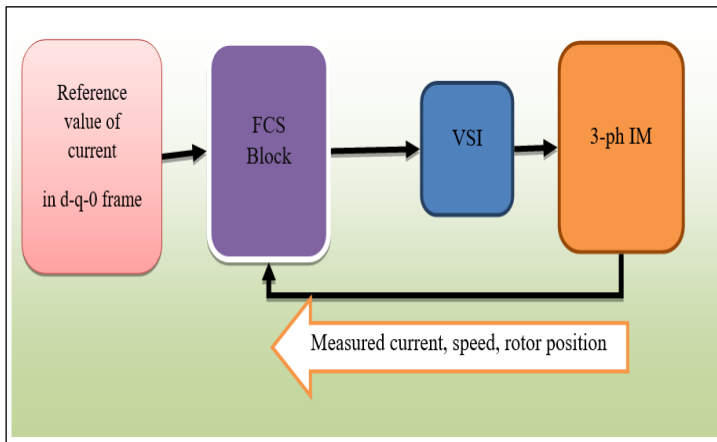


Figure 5: Structure of FCS-MPC for IM.
Source: Authors, (2024).

This method is processed in the following ways.

- 1) The reference value is presented in d-q frame (i_{dref} and i_{qref}).
- 2) Measured currents in d-q frame, speed in radians per second, rotor angular position in radians are used as input to the FCS control block.
- 3) The output of the FCS block, are the switching states to the voltage source inverter.
- 4) The control output of the inverter, as a voltage sources, is fed to the IM model.

In this article a two level three phase VSI is considered for application of predictive schemes. As the overall modelling and computations are in d-q-0 reference frame the voltage vectors generated need to be transformed to d-q-0 coordinate from a-b-c coordinate by means of Park's Transformation.

$$\begin{bmatrix} u_{sd} \\ u_{sq} \end{bmatrix} = \frac{2}{3} \begin{bmatrix} \cos\theta & \cos(\theta - \frac{2\pi}{3}) & \cos(\theta + \frac{2\pi}{3}) \\ -\sin\theta & -\sin(\theta - \frac{2\pi}{3}) & -\sin(\theta + \frac{2\pi}{3}) \end{bmatrix} \begin{bmatrix} V_{an} \\ V_{bn} \\ V_{cn} \end{bmatrix} \quad (21)$$

Where,

u_{sd} = Voltage in d-axis,

u_{sq} = voltage in q-axis,

θ = Rotor position angle

V_{an}, V_{bn}, V_{cn} are the phase voltages of a-b-c with respect to neutral respectively,

V_{dc} = DC voltage supplied to VSI

In FCS-MPC approach, there are seven sets of u_{sd} and u_{sq} values are presented based on the rotor angular position and sampling time. In this control strategy, we deploy the objective function, which is defined as sum of the square of the errors difference, between the desired and predicted current values in d-q frame. The objective function J_k , considers the variables, measured with the sampling time t_i and the manipulated variables $u_{sd}(t_i)$ and $u_{sq}(t_i)$, Equation (16) can be expressed as below :

$$J_k = \left(i_{sd}^*(t_i) - i_{sd}(t_i) - \Delta t \left(-\frac{1}{\tau_\sigma} i_{sd}(t_i) + \omega_s i_{sq}(t_i) + \frac{k_r}{r_\sigma \tau_\sigma \tau_r} \varphi_{rd}(t_i) + \frac{1}{r_\sigma \tau_\sigma} u_{sd}(t_i) \right) \right)^2 + \left(i_{sq}^*(t_i) - i_{sq}(t_i) - \Delta t \left(-\omega_s i_{sd}(t_i) - \frac{1}{\tau_\sigma} i_{sq}(t_i) - \frac{k_r}{r_\sigma \tau_\sigma} \omega_e(t_i) \varphi_{rd}(t_i) + \frac{1}{r_\sigma \tau_\sigma} u_{sq}(t_i) \right) \right)^2 \quad (22)$$

Where

φ_{rd} = rotor flux linkage and k is an index from 0 to 7.

The receding horizon control principle is used here that predicts one step ahead value from the feedback parameters such as $i_{sd}(t_i)$, $i_{sq}(t_i)$, ω_e and θ_e from 3-ph IM model. The objective function is calculated based on the above feedback values, parameters of 3-ph IM model and the pair of $u_{sd} - u_{sq}$ values. Seven sets of objective function are calculated based on seven pairs of $u_{sd} - u_{sq}$ values. The index value is 0 to 7, will be determine with the Previous states of the inverter.

The switching combinations and corresponding voltage vectors imposed in FCS-MPC technique are shown in Table 3.

Table 3: Switching states with voltage vectors of FCS Scheme.

Sa	Sb	Sc	Voltage Vector(v)	V_{an}	V_{bn}	V_{cn}
0	0	0	\vec{v}_0	$-\frac{V_{dc}}{2}$	$-\frac{V_{dc}}{2}$	$-\frac{V_{dc}}{2}$
1	0	0	\vec{v}_1	$\frac{V_{dc}}{2}$	$-\frac{V_{dc}}{2}$	$-\frac{V_{dc}}{2}$
1	1	0	\vec{v}_2	$\frac{V_{dc}}{2}$	$\frac{V_{dc}}{2}$	$-\frac{V_{dc}}{2}$
0	1	0	\vec{v}_3	$-\frac{V_{dc}}{2}$	$\frac{V_{dc}}{2}$	$-\frac{V_{dc}}{2}$
0	1	1	\vec{v}_4	$-\frac{V_{dc}}{2}$	$\frac{V_{dc}}{2}$	$\frac{V_{dc}}{2}$
0	0	1	\vec{v}_5	$-\frac{V_{dc}}{2}$	$-\frac{V_{dc}}{2}$	$\frac{V_{dc}}{2}$
1	0	1	\vec{v}_6	$\frac{V_{dc}}{2}$	$-\frac{V_{dc}}{2}$	$\frac{V_{dc}}{2}$
1	1	1	\vec{v}_7	$\frac{V_{dc}}{2}$	$\frac{V_{dc}}{2}$	$\frac{V_{dc}}{2}$

Source: Authors, (2024).

The phase to neutral voltages of each phase can be defined w.r.t switching states and DC input voltage of inverter as below:

$$\begin{bmatrix} V_{an} \\ V_{bn} \\ V_{cn} \end{bmatrix} = \begin{bmatrix} S_a - \frac{1}{2} \\ S_b - \frac{1}{2} \\ S_c - \frac{1}{2} \end{bmatrix} V_{dc} \quad (23)$$

III.6 PROPOSED IFCS-MPC SCHEME FOR IM

IFCS-MPC method employs the same concept as that of normal FCS-MPC method but the control action is differed such that in I-FCS-MPC method the objective function has variable in terms of voltage signals whereas in normal FCS-MPC method the same has been formed in terms of current signals. The optimal control signals obtained from the feedback control framework is given as

$$\begin{bmatrix} u_{sd}(t_i)^{opt} \\ u_{sq}(t_i)^{opt} \end{bmatrix} = K_{fcs} \left(\begin{bmatrix} i_{sd}^*(t_i) \\ i_{sq}^*(t_i) \end{bmatrix} - \begin{bmatrix} i_{sd}(t_i) \\ i_{sq}(t_i) \end{bmatrix} \right) \quad (24)$$

Where,

K_{fcs} is the gain matrix of the controller and can be extracted from Equation (21) as:

$$K_{fcs}(t_i) = (\Delta t^2 B_m^T B_m)^{-1} B_m^T \Delta t (I + \Delta t A_m(t_i)) \quad (25)$$

Further simplifying by putting the matrix form of A_m & B_m ,

$$K_{fcs}(t_i) = \begin{bmatrix} \frac{r_\sigma \tau_\sigma}{\Delta t} (1 - \frac{\Delta t}{\tau_\sigma}) & \omega_s(t_i) r_\sigma \tau_\sigma \\ -\omega_s(t_i) r_\sigma \tau_\sigma & \frac{r_\sigma \tau_\sigma}{\Delta t} (1 - \frac{\Delta t}{\tau_\sigma}) \end{bmatrix} \quad (26)$$

Using integral action in discrete time control system, Equation (24) can be modified as:

$$\begin{bmatrix} u_{sd}(t_i)^{opt} \\ u_{sq}(t_i)^{opt} \end{bmatrix} = K_{fcs}(t_i) \begin{bmatrix} \frac{K_d}{1-q^{-1}} (i_{sd}^*(t_i) - i_{sd}(t_i)) \\ \frac{K_q}{1-q^{-1}} (i_{sq}^*(t_i) - i_{sq}(t_i)) \\ \begin{bmatrix} i_{sd}(t_i) \\ i_{sq}(t_i) \end{bmatrix} \end{bmatrix} \quad (27)$$

Where 'k_d' and 'k_q' are the value of integral block parameters used for current error at both d-axis and q-axis respectively, $0 < K_d \leq 1$ and $0 < K_q \leq 1$ and $\frac{1}{1-q^{-1}}$ represents functionality of an integrator.

Now at sampling time t_i the optimum control signals are calculated as

$$\begin{bmatrix} u_{sd}(t_i)^{opt} \\ u_{sq}(t_i)^{opt} \end{bmatrix} = \begin{bmatrix} u_{sd}(t_{i-1})^{opt} \\ u_{sq}(t_{i-1})^{opt} \end{bmatrix} + K_{fcs}(t_i) \begin{bmatrix} K_d (i_{sd}^*(t_i) - i_{sd}(t_i)) \\ K_q (i_{sq}^*(t_i) - i_{sq}(t_i)) \end{bmatrix} - K_{fcs}(t_i) \begin{bmatrix} \Delta i_{sd}(t_i) \\ \Delta i_{sq}(t_i) \end{bmatrix} \quad (28)$$

The modified objective function for I-FCS-MPC is given as:

$$J_K = \frac{\Delta t^2}{(r_\sigma \tau_\sigma)^2} (u_{sd}(t_i)^K - u_{sd}(t_i)^{opt})^2 + \frac{\Delta t^2}{(r_\sigma \tau_\sigma)^2} (u_{sq}(t_i)^K - u_{sq}(t_i)^{opt})^2 \quad (29)$$

This is the objective function which is being calculated for each control with index $K = 0, 1, 2, \dots, 6$. The index value and corresponding control set for which the objective function is minimum is selected for the generation of respective switching pulse to the inverter. The schematic of IFCS-MPC for IM have been depicted in figure 6.

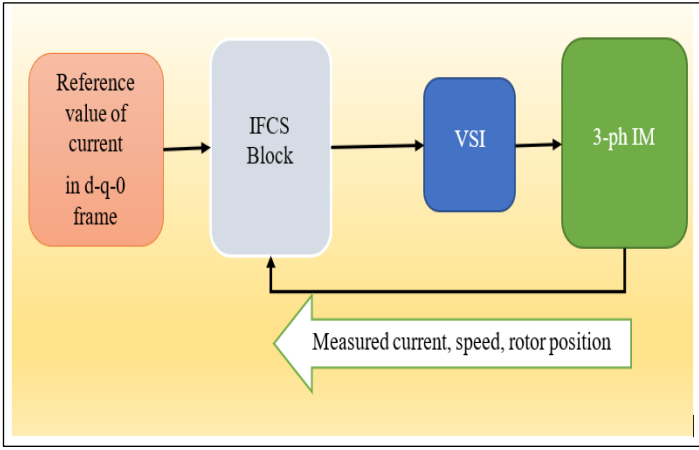


Figure 6: Structure of IFCS-MPC for IM.
Source: Authors, (2024).

The control architecture of I-FCS-MPC for designed three phase induction motor with integral gain parameters and optimal voltage vectors is sited in Figure 7. From the below depicted block diagram we can visualize the control structure of predictive current controller in d-q reference frame. Also it demonstrates the mathematical representation of Equation (27) defined earlier. Further modification with gain parameters, Equation (28) is extracted for optimal evaluation of integral FCS control mechanism. In the implemented control algorithm values of integral gain parameters k_d & k_q are set to be 0.1 [3]. Further analysis can also be done by taking different values of gain parameters between 0 to 1.

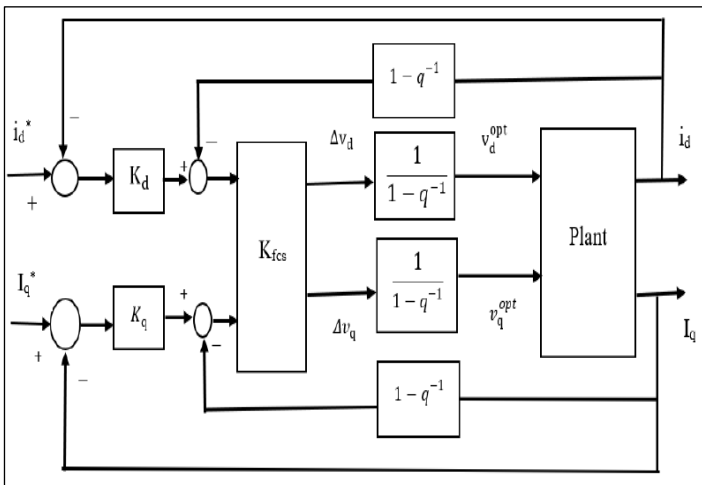


Figure 7: Architecture of Proposed IFCS-MPC.
Source: Authors, (2024).

IV. RESULTS AND DISCUSSIONS

The three phase induction motor with specified parameters mentioned earlier has been modeled and executed with FCS & I-FCS control algorithms applied to inverter circuit. The dynamic characteristics of currents, torque and angular speed of IM have been analyzed for different predictive schemes implemented here. Overall simulation & sampling time are set to be 0.2s and 10μs respectively.

IV.1 CURRENT DYNAMICS ANALYSIS

The reference input current in d-q axis is depicted in Figure 8. From the input current plots it can be seen that d-axis current is taken to be a constant value of $i_{sd}=0.8A$ and q-axis current is

considered to be a step signal of amplitude $i_{sq}=3A$ and changes to 1A at 0.1 sec.

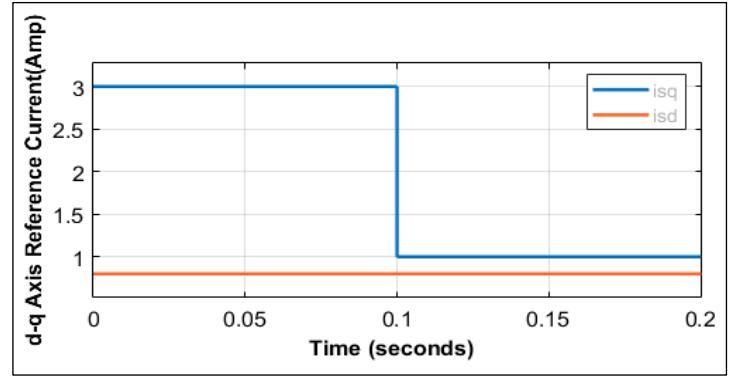


Figure 8: Reference Current in d-q frame
Source: Authors, (2024).

With reference to the d-q axis currents and change in rotor angle (θ), characteristics of desired currents in three phase quantities also change at a particular instant. These currents can be set as a reference to the currents at next execution cycle and it is assumed to be the benchmark for all the proposed approximations. The output currents in d-q and a-b-c forms obtained by FCS MPC techniques are presented in figure 9 and Figure 10 respectively.

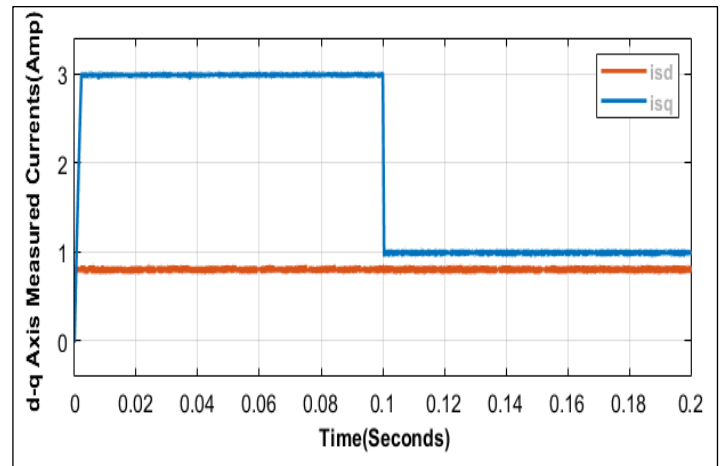


Figure 9: Output Currents of FCS-MPC in d-q frame.
Source: Authors, (2024).

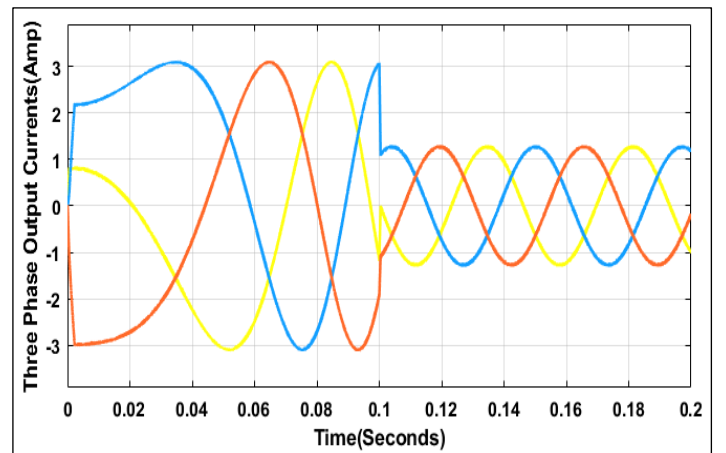


Figure 10: Output Currents of FCS-MPC in abc frame.
Source: Authors, (2024).

In I-FCS-MPC method an integral action is introduced as an outer closed loop for steady state performance enhancement [2],

[10]. The currents obtained by I-FCS action have been presented in both d-q (Figure 11) and a-b-c reference frame (Figure 12).

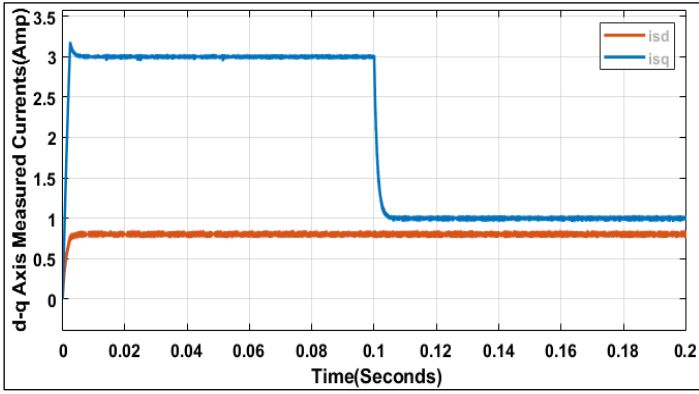


Figure 11: d-q axis currents of I-FCS-MPC Method. Source: Authors, (2024).

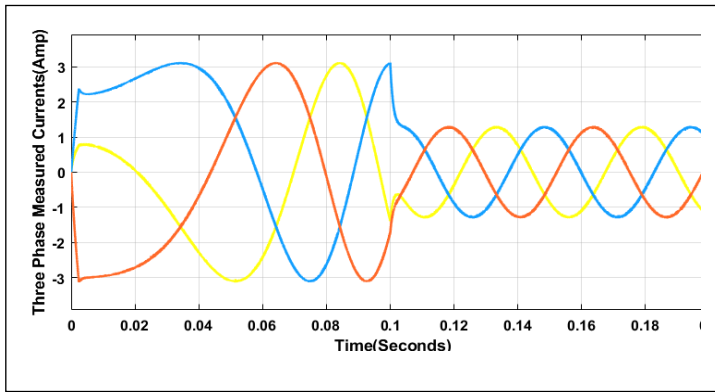


Figure 12: Output Currents of IFCS-MPC Method in abc frame. Source: Authors, (2024).

IV.2 TORQUE DYNAMICS ANALYSIS

From Equation. (11) it can be clearly adopted that electrical torque output (T_e) is a function of quadrature axis current and rotor flux of an induction motor. As a result the behaviour of q-axis current controls the torque characteristics.

The plots of reference load torque (Figure 13) and output torque obtained from FCS and I-FCS predictive control schemes are depicted in Figure 14 & Figure 15 respectively. The applied load torque to the induction motor drive is a step signal of amplitude 2Nm and step change occurs to 1Nm at time 0.1second.

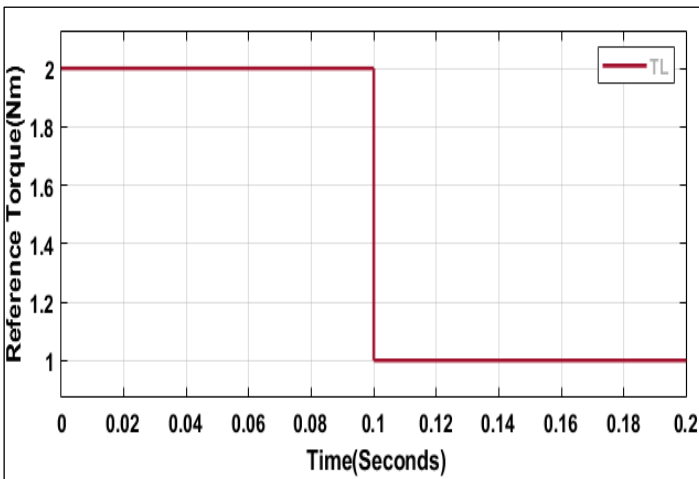


Figure 13: Load torque applied to the 3-ph IM model. Source: Authors, (2024).

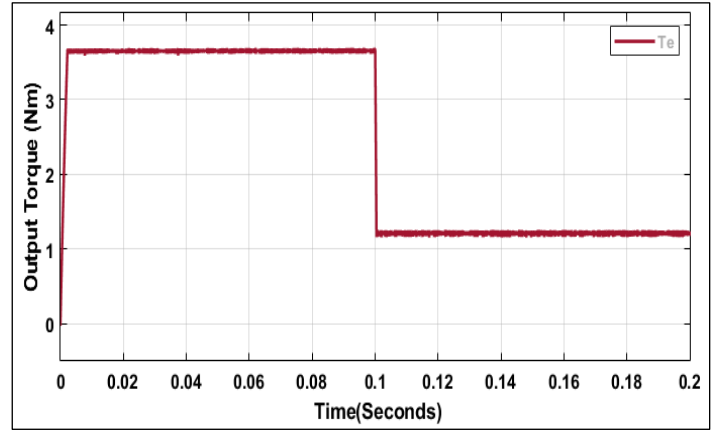


Figure 14: Torque output of FCS-MPC Method. Source: Authors, (2024).

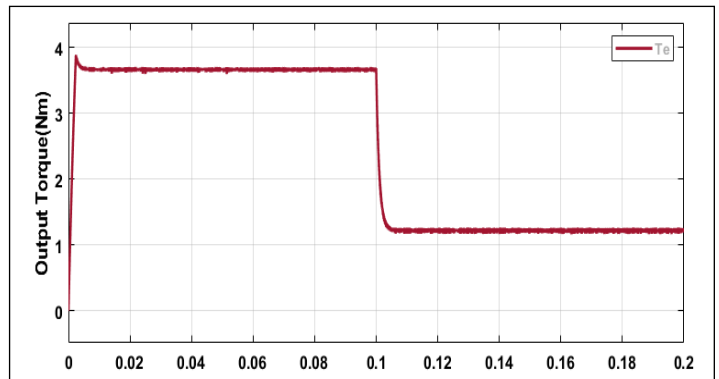


Figure 15: Torque output of IFCS-MPC Method. Source: Authors, (2024).

IV.3 SPEED RESPONSES

As from the earlier analysis we can see that Electromagnetic Torque output, quadrature axis current, rotor flux and angular speed are dependent parameters. Behavioral change of one of the mentioned parameters will deviate the characteristics of others which directly affect the motor performance. Hence By controlling the current we can regulate torque and as a result angular speed of motor also be controlled in coordination with other dependent parameters. This concept can be defined by Equation (13) & (14) mathematically. Angular speed response of induction motor by corresponding step change in load torque and q-axis current for both the proposed predictive controllers are presented below. Figure 16 and Figure 17 respectively demonstrate the angular speed characteristics achieved by FCS & I-FCS control approach.

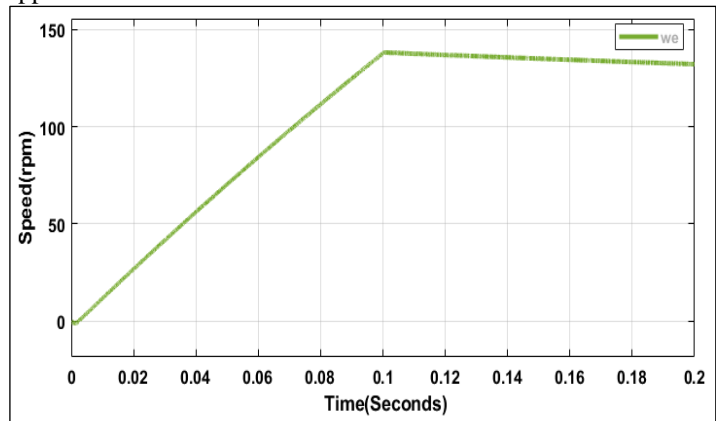


Figure 16: Angular Speed of FCS-MPC Method. Source: Authors, (2024).

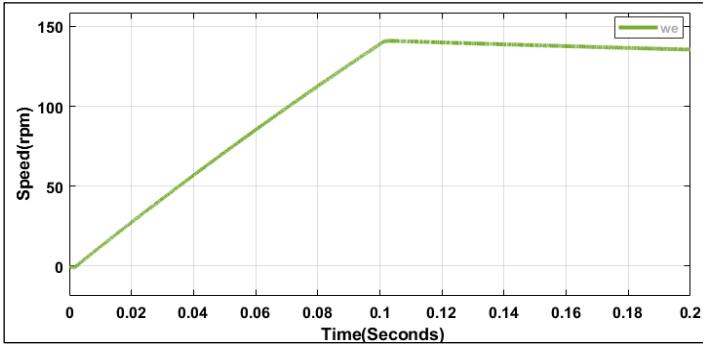


Figure 17: Angular Speed of I-FCS-MPC Method.
Source: Authors, (2024).

The model outputs of currents, torque and angular speed of designed induction motor drive have been captured for the optimum performance evaluation. Current dynamic is studied by a reference step signal of quadrature axis current. Accordingly electromagnetic torque output of the machine also follows the applied step load torque as output torque is a function of q-axis current and rotor flux defined in Equation. (11). As the rotor position angle updates after every time instant, corresponding angular speed also changes. The step responses of current, torque and speed obtained by FCS & IFCS control strategies have been demonstrated here. From the output responses, currents and torque ripples can be visualized.

It can be stated that ripple quantities for both current & torque output are lesser in IFCS-MPC as compared to FCS-MPC.

Similarly slightly more fluctuation is observed in speed response in case of FCS while comparing to integral FCS technique. Based on the model outputs of implemented MPC strategies a performance comparison has been done in terms of peak overshoot, undershoot, settling time, slew rates, rise time & fall time of q-axis current. Overall diagnosis is performed by considering the IM parameters mentioned in Table. 1.

IV.3 COMPARISON OF FCS-MPC AND IFCS-MPC

Simulation of both FCS-MPC and I-FCS-MPC models are implemented with a sampling time of 10 microseconds. Two main factors those determine the characteristics results of the predictive controllers are sampling time and integral gain constants k_d & k_q . Integral gain is applicable only in IFCS-MPC method. For higher value of integral gains, the currents trajectories will overshoot with a good performance in steady state. If we keep the integral gain low, dynamic overshoot can be compensated. Here the value of integral gains are taken as 0.1[3]. Sampling time has not much effect on dynamic performance. Its effect is mostly on steady state ripples. With a higher sampling time the ripple presents are more and hence it is needed to reduce the sampling time. But the computational burden and switching loss of the inverter are restricting the sampling time to fall below certain value. Therefore, a compromise is being made between the ripple allowable and computational time as well as switching loss. Table. 4 shows the quadrature axis characteristics of the proposed controllers based on listed parameters.

Table 4: Quadrature axis Characteristics fo FCS & IFCS

	Measured Parameters	FCS-MPC	IFCS-MPC
Rise Edge	Rise Time (μ s)	1261	1273
	Slew Rate (A/ms)	1.268	1.258
	Preshoot (%)	47.727	52.419
	Overshoot (%)	0.699	8.871
	Undershoot (%)	2.764	2.036
	Settling Time(ms)	119.837	19.901
Fall Edge	Fall Time (μ s)	351.639	1940
	Slew Rate (A/ms)	-4.548	-0.826
	Preshoot (%)	2.786	0.889
	Overshoot (%)	2.04	3.944
	Undershoot (%)	1.214	2.247
	Settling Time(ms)	493.881	19.865

Source: Authors, (2024).

As the IFCS-MPC carries an integral action to compensate for the currents errors as defined in the objective function, Table. 5

illustrates the measured direct and quadrature axis current errors obtained from each of the proposed predictive scheme.

Table 5: Absolute Current Errors measured from the Imposed Predictive Technique

Imposed Predictive Scheme	Absolute Current Error (Amp)		Total Current Error (Amp)
	$ I_{dRef} - I_{dMeas} $	$ I_{qRef} - I_{qMeas} $	
FCS-MPC	00.04037	00.007104	0.047474
IFCS-MPC	00.03069	00.004473	0.035163
Imposed Predictive Scheme	Squared Current Error(Amp)		Total Current Error (Amp)
	$ I_{dRef} - I_{dMeas} $	$ I_{qRef} - I_{qMeas} $	
FCS-MPC	00.00163	55.046e-5	0.00168046
IFCS-MPC	00.0009419	22.001e-5	0.00096191

Source: Authors, (2024).

V. CONCLUSIONS

Induction motor drive has wide range of applications such as in traction, process, production & mining industries. One of the important aspects of these applications is dynamics of electromagnetic torque developed and the voltage fed by the inverter. There are different methods for speed control and torque control like conventional PI, PID & hysteresis controllers. But in case of FCS-MPC method, performance can be improved for non-linear loads effectively due to the predictive nature. Still to improve transient performances, different research papers were proposed. Here a small stride has been done for further improvement in steady state performance of control structures. The torque and the current in q-axis of 3-ph IM are proportional to each other. So, throughout the control approach both the reference current in q-axis and the reference load torque are applied as step function to observe the dynamic behaviour of 3-ph IM. The performance of MPC coordinated schemes applied to IM drive is evaluated. Operating principle of proposed predictive controllers differ by their mode of control actions. Applied FCS & I-FCS strategies have specified control approach based on defined objective functions. Peak Overshoot, undershoot, preshoot, settling time & slew rates of quadrature current of IM subjected to step change are analyzed and thus the dynamic control characteristics of implemented control techniques have been diagnosed. FCS & I-FCS have almost similar control strategy but IFCS has the inherent features of reducing steady state errors and improving slew rates. Also I-FCS possesses better current & torque responses with minimum ripples and superior trajectories w.r.t step i/p signal. There is not much difference in speed responses of both FCS & I-FCS MPC except the later has slightly less ripples as compared to FCS-MPC.

All these performed predictive aspects provide a genuine control algorithm for flexible and reliable implementations. The adaptive nature of MPC methods has tremendous skills of being a superior controller in modern control dilemma. Furthermore, many initiatives such as harmonics & speed controls and switching power loss reduction of inverters by MPC based schemes can be designed. Also in extension predictive control approach can be milestone research for Electric vehicles, FACTS devices and in various power system control measures.

VI. AUTHOR'S CONTRIBUTION

Conceptualization: Shaswat Chirantan and Bibhuti Bhusan Pati

Methodology: Shaswat Chirantan and Bibhuti Bhusan Pati

Investigation: Shaswat Chirantan and Bibhuti Bhusan Pati

Discussion of results: Shaswat Chirantan and Bibhuti Bhusan Pati

Writing – Original Draft: Shaswat Chirantan and Bibhuti Bhusan Pati

Writing – Review and Editing: Shaswat Chirantan and Bibhuti Bhusan Pati

Resources: Shaswat Chirantan and Bibhuti Bhusan Pati

Supervision: Shaswat Chirantan and Bibhuti Bhusan Pati

Approval of the final text: Shaswat Chirantan and Bibhuti Bhusan Pati

VIII. REFERENCES

[1] Rodriguez, J. and Cortes, P.: "Predictive Control of Power Converters and Electrical Drives", John Wiley & Sons Ltd, United Kingdom, (2012)

[2] Wang L, Gan L. "Integral FCS predictive current control of induction motor drive. IFAC Proceedings Volumes". 2014 Jan 1;47(3):pp. 11956-11961.

[3] Wang L, Chai S, Yoo D, Gan L, Ng K. "PID and predictive control of electrical drives and power converters using MATLAB/Simulink". JohnWiley & Sons; 2015 Mar 2. pp. 171-205.

[4] Odhano S, Bojoi R, Formentini A, Zanchetta P, Tenconi A. "Direct flux and current vector control for induction motor drives using model predictive control theory". IET Electric Power Applications. 2017 Sep 4;11(8): pp. 1483-1491.

[5] Ahmed A.A., Koh, B.K., Kim, J.S. and Lee, Y.I., (2017). "Finite control set-model predictive speed control for induction motors with optimal duration". Proc. IFAC Papers On Line, Vol. 50(1), pp.7801-7806.

[6] Zhu B, Rajashekara K, Kubo H. "Comparison between current-based and flux/torque-based model predictive control methods for open-end winding induction motor drives". IET Electric Power Applications. 2017 Sep 4;11(8):pp. 1397-1406.

[7] Wang F, Zhang Z, Mei X, Rodriguez J, Kennel R. "Advanced control strategies of induction machine: Field oriented control, direct torque control and model predictive control". Energies. 2018 Jan;11(1):1-13.

[8] Norambuena M, Rodriguez J, Zhang Z, Wang F, Garcia C, Kennel R. "A very simple strategy for high-quality performance of AC machines using model predictive control". IEEE Transactions on Power Electronics. 2018 Mar 9;34(1):pp. 794-800.

[9] Rubino S, Bojoi R, Odhano SA, Zanchetta P. "Model predictive direct flux vector control of multi-three-phase induction motor drives". IEEE Transactions on Industry Applications. 2018 Apr 23;54(5):pp 4394-4404.

[10] Ramirez RO, Espinoza JR, Baier CR, Rivera M, Villarreal F, Guzman JI, Melin PE. "Finite-state model predictive control with integral action applied to a single phase Z-source inverter". IEEE Journal of Emerging and Selected Topics in Power Electronics. 2018 Sep 18;7(1):pp. 228-239.

[11] Karamanakos P, Geyer T. "Guidelines for the design of finite control set model predictive controllers". IEEE Transactions on Power Electronics. 2019 Nov 19;35(7):pp. 7434-7450.

[12] Wróbel, Karol Tomasz, Krzysztof Szabat, and Piotr Serkies. "Long-horizon model predictive control of induction motor drive." Archives of Electrical Engineering (2019): 579-593.

[13] Stando D, Kazmierkowski MP. Constant switching frequency predictive control scheme for three-level inverter-fed sensorless induction motor drive. Bulletin of the Polish Academy of Sciences. Technical Sciences. 2020;68(5).

[14] Wang, Junxiao, and Fengxiang Wang. "Robust sensor less FCS-PCC control for inverter-based induction machine systems with high-order disturbance compensation". Journal of Power Electronics (2020): pp. 1222-1231.

[15] Ortombina L, Karamanakos P, Zigliotto M. "Robustness Analysis of Long-Horizon Direct Model Predictive Control: Induction Motor Drives". IEEE 21st Workshop on Control and Modeling for Power Electronics (COMPEL) 2020 Nov 9 (pp. 1-8).

[16] Zhang, Yanqing, Zhonggang Yin, Wei Li, Jing Liu, and Yanping Zhang. "Adaptive sliding-mode-based speed control in finite control set model predictive torque control for induction motors." IEEE Transactions on Power Electronics 36, no. 7 (2020): 8076-8087.

[17] Kiani B, Mozafari B, Soleymani S, Mohammadnezhad Shourkaei H. Predictive torque control of induction motor drive with reduction of torque and flux ripple. Bulletin of the Polish Academy of Sciences. Technical Sciences. 2021;69(4).

[18] Ali, Anmar Kh, and Riyadh G. Omar. "Finite control set model predictive direct current control strategy with constraints applying to drive three-phase induction motor". International Journal of Electrical & Computer Engineering (2088-8708) (2021) vol.11(4) pp 1-9.

[19] Ayala, Magno, Jesus Doval-Gandoy, Osvaldo Gonzalez, Jorge Rodas, Raul Gregor, and Marco Rivera. "Experimental stability study of modulated model predictive current controllers applied to six-phase induction motor drives." IEEE Transactions on Power Electronics 36, no. 11 (2021): 13275-13284.

[20] Bhowate, Apekshit, Mohan V. Aware, and Sohith Sharma. "Predictive Torque Control of Five-Phase Induction Motor Drive Using Successive Cost Functions for CMV Elimination." IEEE Transactions on Power Electronics 36, no. 12 (2021): 14133-14141.

- [21] Shawier, Abdullah, Abdelrahman Habib, Mohamed Mamdouh, Ayman Samy Abdel-Khalik, and Khaled H. Ahmed. "Assessment of predictive current control of six-phase induction motor with different winding configurations." *IEEE Access* 9 (2021): 81125-81138.
- [22] Fereidooni, Arash, S. Alireza Davari, Cristian Garcia, and Jose Rodriguez. "Simplified Predictive Stator Current Phase Angle Control of Induction Motor With a Reference Manipulation Technique." *IEEE Access* 9 (2021): 54173-54183.
- [23] Bassi, Hussain, Muhyaddin Jamal Hosin Rawa, M. Abbas Abbasi, Abdul Rashid Husain, Nik Rumzi Nik Idris, and Waqas Anjum. "Predictive flux control for induction motor drives with modified disturbance observer for improved transient response." U.S. Patent 11,031,891, issued June 8, 2021.
- [24] Zhang, Yongchang, Xing Wang, Haitao Yang, Boyue Zhang, and Jose Rodriguez. "Robust predictive current control of induction motors based on linear extended state observer." *Chinese Journal of Electrical Engineering* 7, no. 1 (2021): 94-105.
- [25] Mousavi, Mahdi S., S. Alireza Davari, Vahab Nekoukar, Cristian Garcia, and Jose Rodriguez. "Integral Sliding Mode Observer-Based Ultra-Local Model for Finite-Set Model Predictive Current Control of Induction Motor." *IEEE Journal of Emerging and Selected Topics in Power Electronics* (2021).
- [26] Kiani, Babak. "A computationally low burden MPTC of induction machine without prediction loop and weighting factor." *Bulletin of the Polish Academy of Sciences: Technical Sciences* (2022): e142050-e142050
- [27] Rodriguez, Jose, Cristian Garcia, Andres Mora, Freddy Flores-Bahamonde, Pablo Acuna, Mateja Novak, Yongchang Zhang et al. "Latest Advances of Model Predictive Control in Electrical Drives—Part I: Basic Concepts and Advanced Strategies." *IEEE Transactions on Power Electronics* 37, no. 4 (2021): 3927-3942.
- [28] Rodriguez, Jose, Cristian Garcia, Andres Mora, S. Alireza Davari, Jorge Rodas, Diego Fernando Valencia, Mahmoud Elmorschedy et al. "Latest advances of model predictive control in electrical drives—Part II: Applications and benchmarking with classical control methods." *IEEE Transactions on Power Electronics* 37, no. 5 (2021): 5047-5061.
- [29] Mousavi, Mahdi S., S. Alireza Davari, Vahab Nekoukar, Cristian Garcia, and Jose Rodriguez. "Finite-Set Model Predictive Current Control of Induction Motors by Direct Use of Total Disturbance." *IEEE Access* 9 (2021): 107779-107790.
- [30] Mamdouh, Mohamed, Ayman Samy Abdel-Khalik, and Mohamed A. Abido. "Predictive current control of asymmetrical six-phase induction motor without weighting factors." *Alexandria Engineering Journal* 61, no. 5 (2022): 3793-3803.
- [31] Habib, Abdelrahman, Abdullah Shawier, M. Mamdouh, Ayman Samy Abdel-Khalik, Mostafa S. Hamad, and Shehab Ahmed. "Predictive current control-based pseudo six-phase induction motor drive." *Alexandria Engineering Journal* 61, no. 5 (2022): 3937-3948
- [32] R. Houili, M. Y. Hammoudi, A. Betka and A. Titaouine, "Stochastic optimization algorithms for parameter identification of three phase induction motors with experimental verification," 2023 International Conference on Advances in Electronics, Control and Communication Systems (ICAEECCS), BLIDA, Algeria, 2023, pp. 1-6.
- [33] El Ouanjli, Najib, Said Mahfoud, Ameena Saad Al-Sumaiti, Soukaina El Daoudi, Aziz Derouich, Mohammed El Mahfoud, and Mahmoud A. Mossa. "Improved twelve sectors DTC strategy of induction motor drive using Backstepping speed controller and P-MRAS stator resistance identification-design and validation." *Alexandria Engineering Journal* 80 (2023): 358-371.
- [34] Z. Liu, Y. Han, G. Feng and N. C. Kar, "Efficient Nonlinear Multi-Parameter Decoupled Estimation of PMSM Drives Based on Multi-State Voltage and Torque Measurements," in *IEEE Transactions on Energy Conversion*, vol. 38, no. 1, pp. 321-331, March 2023, doi: 10.1109/TEC.2022.3187130.
- [35] J. Cui, T. Tao and W. Zhao, "Optimized Control Set Model Predictive Control for Dual Three-Phase PMSM With Minimum Error Duty Cycle Regulation," in *IEEE Transactions on Power Electronics*, vol. 39, no. 1, pp. 1319-1332, Jan. 2024, doi: 10.1109/TPEL.2023.3324209
- [36] Chirantan, Shaswat, and Bibhuti Bhusan Pati. "Torque and dq axis current dynamics of an inverter fed induction motor drive that leverages computational intelligent techniques." *AIMS Electronics and Electrical Engineering* 8, no. 1 (2024): 28-52.